nature neuroscience

miR-132, an experience-dependent microRNA, is essential for visual cortex plasticity

Nikolaos Mellios[1,5], Hiroki Sugihara[1,5], Jorge Castro[1], Abhishek Banerjee[1], Chuong Le[1], Arooshi Kumar[1], Benjamin Crawford[1], Julia Strathmann[2], Daniela Tropea[1,4], Stuart S Levine[3], Dieter Edbauer[2] & Mriganka Sur[1]

Using quantitative analyses, we identified microRNAs (miRNAs) that were abundantly expressed in visual cortex and that responded to dark rearing and/or monocular deprivation. The most substantially altered miRNA, miR-132, was rapidly upregulated after eye opening and was delayed by dark rearing. *In vivo* inhibition of miR-132 in mice prevented ocular dominance plasticity in identified neurons following monocular deprivation and affected the maturation of dendritic spines, demonstrating its critical role in the plasticity of visual cortex circuits.

miRNAs are small, noncoding RNAs that are known to orchestrate the expression of protein-coding genes[1]. They are particularly enriched in the nervous system and have been shown to influence neuronal development and function[2–4]. However, little is known about their role in experience-dependent cortical plasticity. We used molecular analyses to examine changes in the expression of miRNAs in the primary visual cortex (V1) of mice that were visually deprived[5,6], either by dark rearing, with complete absence of light from birth, or by monocular deprivation, with suture of one eyelid during the critical period of heightened ocular dominance plasticity[7]. The expression of a subset of miRNAs was substantially altered by visual deprivation. Using structural and functional analyses, we found that the most robustly experience-dependent miRNA, miR-132, is a crucial regulator of visual cortex plasticity.

To screen for miRNAs that respond to visual deprivation, we compared their expression in RNA extracted from V1 of three groups of mice that were age-matched to the peak of the critical period[5]: postnatal day 28 (P28) control mice reared with a normal light/dark cycle, P28 mice reared in darkness from birth, and P28 monocularly deprived mice, reared with their eyelid sutured from P24–28 (**Supplementary Methods** and **Supplementary Fig. 1**). All animal experiments were approved by the Massachusetts Institute of Technology Institutional Animal Care and Use Committee. Statistical analysis of microarray data[8] revealed 21 differentially expressed miRNAs, the majority of which were affected in a similar manner by dark rearing and monocular deprivation (**Supplementary Figs. 1–3** and **Supplementary Table 1**). We then used mature miRNA-specific quantitative real-time PCR (qRT-PCR) to examine a larger set of dark-rearing and monocular deprivation samples and independently detected 19 of the miRNAs that were differentially expressed in the microarray (**Fig. 1a**). Overall, our miRNA qRT-PCR and microarray results were significantly correlated ($P < 0.0001$) (**Supplementary Fig. 4a**). qRT-PCR confirmed the altered expression of nine miRNAs, with decreases in miR-132, miR-212 and miR-690 and increases in miR-497 and miR-551b expression being observed after both dark rearing (miR-132, $P < 0.0001$; miR-212, $P = 0.0010$; miR-690, $P = 0.0245$; miR-497, $P = 0.0432$; miR-551b, $P = 0.0489$) and monocular deprivation (miR-132, $P = 0.0004$; miR-212, $P = 0.0139$; miR-690, $P = 0.0245$; miR-497, $P = 0.0337$; miR-551b, $P = 0.0264$) (**Fig. 1a**). Expression of two control brain-enriched miRNAs (miR-124a and miR-125b) was unaffected, consistent with our microarray results (**Fig. 1a**). Furthermore, no significant changes ($P > 0.10$) were observed in the ipsilateral V1 areas of monocular deprivation–altered miRNAs (**Supplementary Fig. 4b**). In addition, qRT-PCR of primary miRNA precursors (pri-miRNAs) indicated that their changes mirrored those of six out of nine mature miRNAs, which is suggestive of a transcriptional mechanism (**Supplementary Fig. 5**). We also combined *in silico* miRNA target prediction and pathway analysis and found that multiple pathways linked to synaptic plasticity were predicted to be highly targeted by experience-dependent miRNAs (**Supplementary Tables 2** and **3**). Thus, our microarray and qRT-PCR analyses revealed a set of miRNAs in V1 that are reliably regulated by visual experience and are predicted to target plasticity-related molecular pathways.

Focusing on the most highly affected miRNA, miR-132, we found, using qRT-PCR, that it was robustly increased after eye opening and through the critical period for ocular dominance plasticity, and that its diminished expression after dark rearing was gradually normalized after light exposure (**Fig. 1b**). Furthermore, using locked nucleic acid (LNA) *in situ* hybridization, we found that expression of miR-132 was reduced in cortical layers 2–4 of V1 after both dark rearing and monocular deprivation (**Fig. 1c**,**d** and **Supplementary Figs. 6** and **7**), which are sites of rapid ocular dominance plasticity[9]. Given these observations, we reasoned that miR-132 is well positioned to orchestrate the molecular components of experience-dependent plasticity in V1.

To manipulate miR-132 function *in vivo*, we injected wild-type or GFP-S mice with a mCherry–miR-132 competitive inhibitor (sponge)–expressing lentivirus that predominantly infects neurons and results in specific 'sequestering' of endogenous miR-132 (refs. 4,10) (**Supplementary Fig. 8**). We then measured the expression of p250GAP, a GTPase that is targeted by miR-132 and is known to affect spine growth and morphology[11–13], and examined structural changes in transfected pyramidal neurons at P28. We found increased p250GAP in mCherry–miR-132 sponge–expressing pyramidal

[1]Department of Brain and Cognitive Sciences, Picower Institute for Learning and Memory, Massachusetts Institute of Technology, Cambridge, Massachusetts, USA. [2]DZNE - German Center for Neurodegenerative Diseases, Munich, Germany. [3]Biomicro Center, Massachusetts Institute of Technology, Cambridge, Massachusetts, USA. [4]Present address: Trinity College Dublin, St. James Hospital, Dublin, Ireland. [5]These authors contributed equally to this work. Correspondence should be addressed to M.S. (msur@mit.edu).

Received 23 May; accepted 6 July; published online 4 September 2011; doi:10.1038/nn.2909

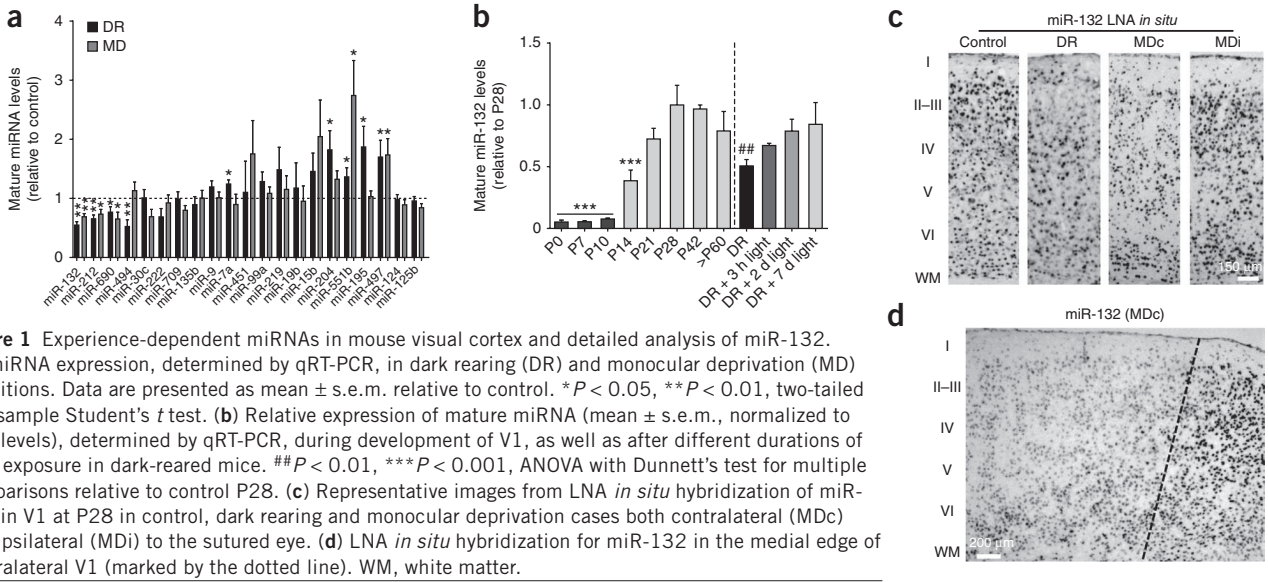

Figure 1 Experience-dependent miRNAs in mouse visual cortex and detailed analysis of miR-132. (**a**) miRNA expression, determined by qRT-PCR, in dark rearing (DR) and monocular deprivation (MD) conditions. Data are presented as mean ± s.e.m. relative to control. $^{*}P < 0.05$, $^{**}P < 0.01$, two-tailed one-sample Student's *t* test. (**b**) Relative expression of mature miRNA (mean ± s.e.m., normalized to P28 levels), determined by qRT-PCR, during development of V1, as well as after different durations of light exposure in dark-reared mice. $^{\#\#}P < 0.01$, $^{***}P < 0.001$, ANOVA with Dunnett's test for multiple comparisons relative to control P28. (**c**) Representative images from LNA *in situ* hybridization of miR-132 in V1 at P28 in control, dark rearing and monocular deprivation cases both contralateral (MDc) and ipsilateral (MDi) to the sutured eye. (**d**) LNA *in situ* hybridization for miR-132 in the medial edge of contralateral V1 (marked by the dotted line). WM, white matter.

neurons and reduced spine density (mean ± s.e.m., 0.3025 ± 0.0213 spines per μm for sponge-infected versus 0.4508 ± 0.0357 spines per μm for control neurons, $P = 0.0385$, two-tailed Student's *t* test), despite the neuronal size and arborization of the sponge-infected neurons remaining normal after both P5 and P16 injections (**Fig. 2a–h** and **Supplementary Fig. 9a–h).** Examination of the changes in spine morphology revealed that miR-132 inhibition resulted in more immature spines (**Fig. 2i** and **Supplementary Fig. 9i**), mainly by reducing the percentage of mushroom spines and increasing the proportion of immature filopodia (**Supplementary Fig. 9j**). We assayed for accompanying physiological synaptic changes in sponge-infected neurons by measuring AMPA receptor–dependent spontaneous miniature excitatory postsynaptic currents (mEPSCs), using whole-cell recordings from layer 2/3 pyramidal neurons (**Fig. 2j** and **Supplementary Fig. 10**). We found no change in mEPSC frequency, but there was a significant reduction in mEPSC amplitude in sponge-infected neurons ($P = 0.0385$) (**Fig. 2j**). These effects of miR-132 inhibition are consistent with delayed synaptic maturation of pyramidal V1 neurons.

To directly examine the influence of miR-132 on ocular dominance plasticity, we used two-photon calcium imaging to measure the strength of neuronal responses to contralateral and ipsilateral eye stimulation in the binocular area of V1, contralateral to the deprived eye, following neonatal injection of mCherry–miR-132 sponge–expressing virus (**Fig. 3a**). The relative strength of contralateral eye– and ipsilateral eye–driven responses was quantified by calculating the ocular dominance index (ODI) for each neuron (**Fig. 3b**). We found that *in vivo* miR-132 inhibition disrupted the ocular dominance shift that was normally present after 4 d of monocular deprivation (**Fig. 3c**,**d**). Analysis of eye-specific responses revealed that the observed blockade of plasticity was mainly due to prevention of monocular deprivation

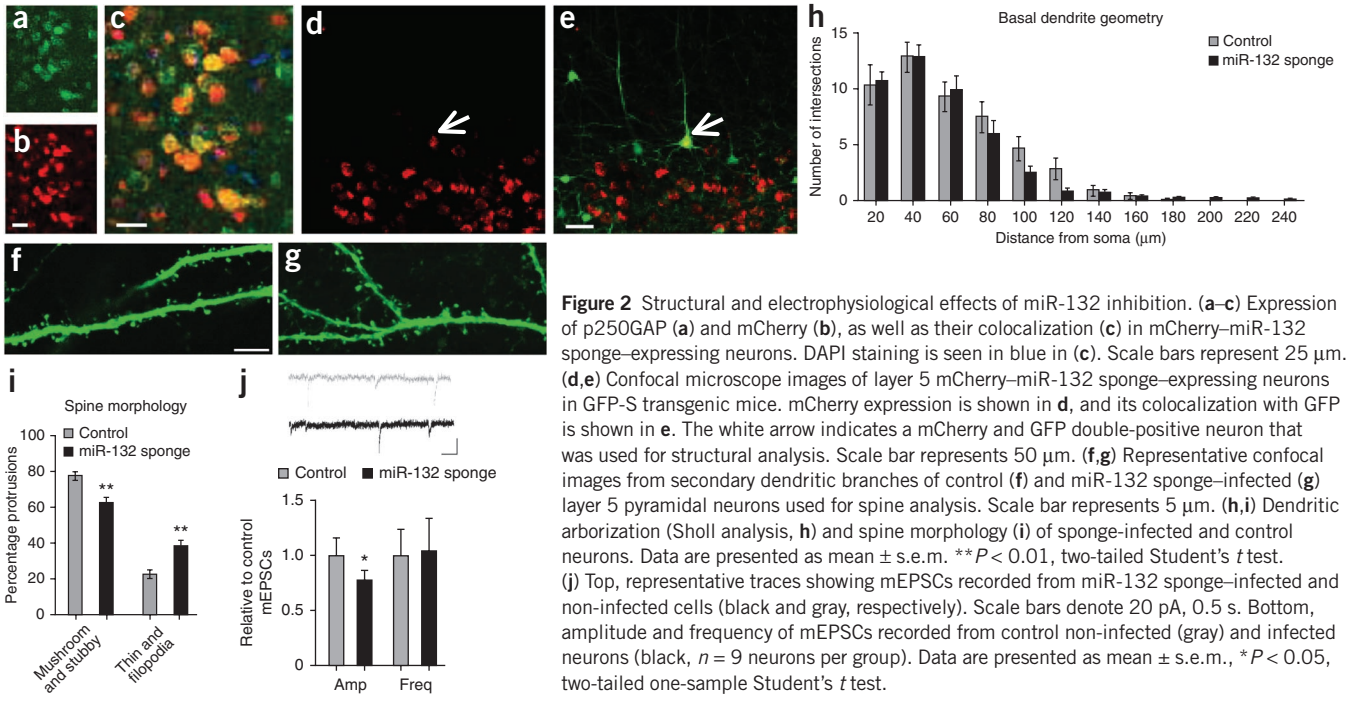

Figure 2 Structural and electrophysiological effects of miR-132 inhibition. (**a**–**c**) Expression of p250GAP (**a**) and mCherry (**b**), as well as their colocalization (**c**) in mCherry–miR-132 sponge–expressing neurons. DAPI staining is seen in blue in (**c**). Scale bars represent 25 μm. (**d**,**e**) Confocal microscope images of layer 5 mCherry–miR-132 sponge–expressing neurons in GFP-S transgenic mice. mCherry expression is shown in **d**, and its colocalization with GFP is shown in **e**. The white arrow indicates a mCherry and GFP double-positive neuron that was used for structural analysis. Scale bar represents 50 μm. (**f**,**g**) Representative confocal images from secondary dendritic branches of control (**f**) and miR-132 sponge–infected (**g**) layer 5 pyramidal neurons used for spine analysis. Scale bar represents 5 μm. (**h**,**i**) Dendritic arborization (Sholl analysis, **h**) and spine morphology (**i**) of sponge-infected and control neurons. Data are presented as mean ± s.e.m. $^{**}P < 0.01$, two-tailed Student's *t* test. (**j**) Top, representative traces showing mEPSCs recorded from miR-132 sponge–infected and non-infected cells (black and gray, respectively). Scale bars denote 20 pA, 0.5 s. Bottom, amplitude and frequency of mEPSCs recorded from control non-infected (gray) and infected neurons (black, $n = 9$ neurons per group). Data are presented as mean ± s.e.m., $^{*}P < 0.05$, two-tailed one-sample Student's *t* test.

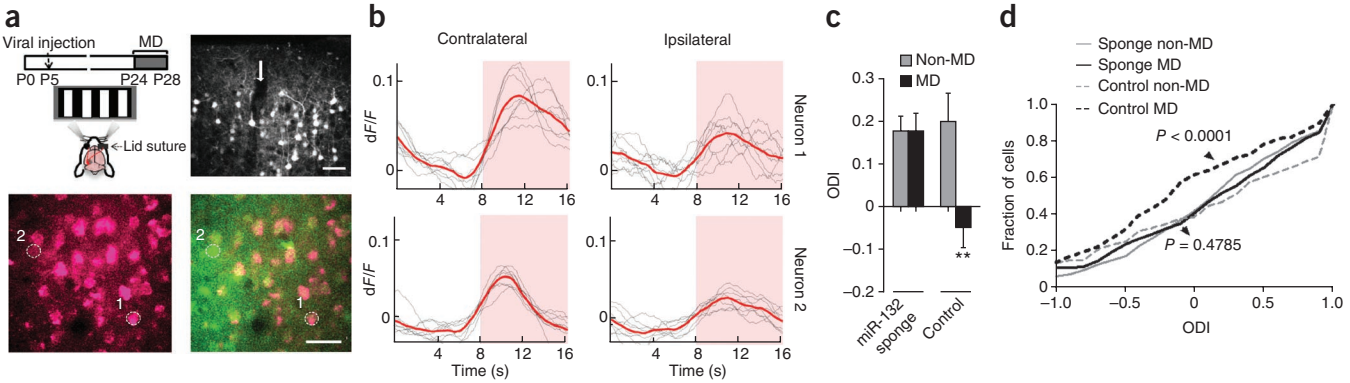

Figure 3 *In vivo* inhibition of miR-132 in V1 neurons disrupts their ocular dominance plasticity. (**a**) Top left, schematic of experimental design. Top right, confocal microscopy images showing mCherry expression in cortical layers 1–3 at P28 following neonatal injection (arrow) of mCherry–miR-132 sponge–expressing lentivirus. Bottom, two-photon microscopy image showing mCherry expression alone (left) and its overlay with OGB (green) fluorescence (right) in an injected mouse that underwent monocular deprivation; selected neurons used in **b** are circled and numbered. Scale bars represent 40 µm. (**b**) Example of contralateral eye– and ipsilateral eye–driven calcium responses of the neurons shown in **a** that express high (neuron 1) or low (neuron 2) levels of mCherry–miR-132 sponge. Pink shaded area indicates period with visual stimulus. Calculated ODIs were 0.73 (neuron 1) and 0.55 (neuron 2). (**c**) ODI values (ODI = (contralateral – ipsilateral) / (contralateral + ipsilateral); mean ± s.e.m.) derived from peak visual responses obtained by two-photon calcium imaging in mice injected with mCherry–miR-132 sponge–expressing lentivirus. Black bars indicate mice subjected to 4 d of monocular deprivation and light gray bars indicate mice that were not subjected to monocular deprivation (miR-132 sponge non–monocular deprivation, five mice, 290 neurons; miR-132 sponge monocular deprivation, four mice, 232 neurons; control non–monocular deprivation; three mice, 120 neurons; control monocular deprivation, three mice, 177 neurons). The ODI did not shift following monocular deprivation in mice that were injected with miR-132 sponge, but not control, virus. A significantly larger ocular dominance shift was seen in control monocularly deprived mice than in any of the other conditions (**$P < 0.01$, Mann-Whitney test comparing neurons; $P < 0.05$ treating each mouse as a single datum). (**d**) Cumulative histogram of ODI data shown in **c**. There was a significant difference between control monocular deprivation and non–monocular deprivation neurons (black and light gray dashed lines, respectively), but not between miR-132 sponge–infected monocular deprivation and non–monocular deprivation neurons (black and light gray lines, respectively) (Kolmogorov-Smirnov test).

effects on contralateral responses (**Supplementary Figs. 11** and **12**). As expected, neurons that were transfected with the control virus (containing mCherry without the miR-132 sponge sequence) did show a shift in ocular dominance toward the undeprived eye (**Fig. 3c**,**d**). Notably, neurons expressing low levels of miR-132 sponge (as judged by mCherry load) that were present in the proximity of neurons expressing higher levels displayed a shift in their ODI that was comparable to that of control monocularly deprived animals (**Supplementary Fig. 13a–d**), as did uninfected neurons that were located adjacent to sponge-infected ones (**Supplementary Fig. 13e**), suggesting a potential threshold for the degree of miR-132 inhibition needed to abrogate ocular dominance plasticity. Thus, miR-132 expression in V1 neurons is essential for plasticity of their responses and underlying circuits.

Ocular dominance plasticity following monocular deprivation during the critical period leads to coordinated changes in the functional responses of neurons and structural properties of spines[7,14,15]. Given that miR-132 is upregulated after eye opening in a time window that parallels the critical period and that dark rearing prevents this upregulation, we hypothesize that light-induced, and thus activity-induced, elevation of miR-132 expression is crucial for the initiation of ocular dominance plasticity. Indeed, sequestering miR-132 levels before eye opening and extending through the critical period prevented both monocular deprivation–induced functional plasticity and structural maturation of spines. The failure of miR-132 sponge–expressing neurons to exhibit ocular dominance plasticity at P28 likely reflects a shift of the critical period to a later age, effectively by maintaining the cortex in a earlier developmental stage (see also **Supplementary Discussion**). We conclude that experience-dependent upregulation of miR-132 contributes fundamentally to the sensitive period of cortical plasticity.

Accession codes. Gene Expression Omnibus: GSE31536.

Note: Supplementary information is available on the Nature Neuroscience website.

ACKNOWLEDGMENTS

We thank J. Sharma and C. Runyan for feedback, G. Kreiman for assistance with data analysis, M. Constantine-Paton and her laboratory for sharing equipment and B. Karki for technical assistance. Supported by US National Eye Institute Ruth L. Kirschstein Postdoctoral Fellowship 1F32EY020066-01 (N.M.), Helmholtz Young Investigator program HZ-NG-607 (D.E.), a Simons Foundation postdoctoral fellowship (A.B.) and US National Institutes of Health EY017098 and EY007023 to M.S.

AUTHOR CONTRIBUTIONS

N.M. conceived the hypothesis, designed and executed experiments, analyzed the data, and wrote the manuscript. H.S. conducted *in vivo* two-photon calcium imaging and analyzed the related data. J.C. conducted neonatal virus injections and structural analysis. A.B. carried out slice electrophysiology. A.B., C.L., A.K., B.C., J.C. and D.T. assisted in various experiments, data analysis and figure preparation. J.S. and D.E. constructed and tested lentivirus vectors and S.S.L. performed miRNA microarray experiments. M.S. supervised and orchestrated all of the experiments and wrote the manuscript with N.M.

COMPETING FINANCIAL INTERESTS

The authors declare no competing financial interests.

Published online at http://www.nature.com/natureneuroscience/.
Reprints and permissions information is available online at http://www.nature.com/reprints/index.html.

1. Bartel, D.P. *Cell* **116**, 281–297 (2004).
2. Giraldez, A.J. *et al. Science* **308**, 833–838 (2005).
3. Schratt, G.M. *et al. Nature* **439**, 283–289 (2006).
4. Edbauer, D. *et al. Neuron* **65**, 373–384 (2010).
5. Gordon, J.A. & Stryker, M.P. *J. Neurosci.* **16**, 3274–3286 (1996).
6. Frenkel, M.Y. & Bear, M.F. *Neuron* **44**, 917–923 (2004).
7. Hensch, T.K. *Nat. Rev. Neurosci.* **6**, 877–888 (2005).
8. Tusher, V.G., Tibshiran, R. & Chu, G. *Proc. Natl. Acad. Sci. USA* **98**, 5116–5121 (2001).
9. Trachtenberg, J.T., Trepel, C. & Stryker, M.P. *Science* **287**, 2029–2032 (2000).
10. Ebert, M.S., Neilson, J.R. & Sharp, P.A. *Nat. Methods* **4**, 721–726 (2007).
11. Vo, N. *et al. Proc. Natl. Acad. Sci. USA* **102**, 16426–16431 (2005).
12. Wayman, G.A. *et al. Proc. Natl. Acad. Sci. USA* **105**, 9093–9098 (2008).
13. Impey, S. *et al. Mol. Cell. Neurosci.* **43**, 146–156 (2010).
14. Mataga, N., Mizuguchi, Y. & Hensch, T.K. *Neuron* **44**, 1031–1041 (2004).
15. Oray, S., Majewska, A. & Sur, M. *Neuron* **44**, 1021–1030 (2004).